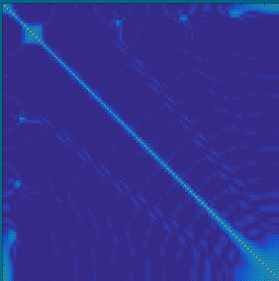


# Optimal Control of Spin Systems

Newton-GRAPE



David L. Goodwin,  
& Ilya Kuprov

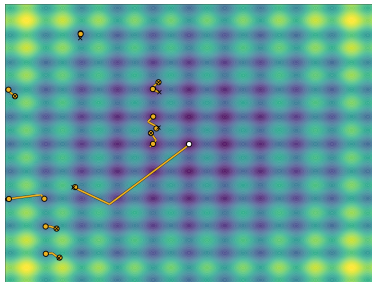
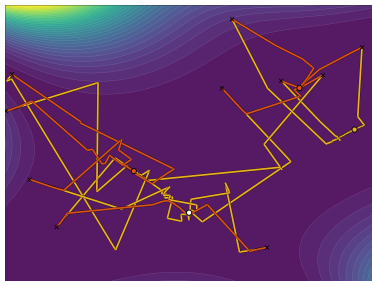
d.goodwin@soton.ac.uk

Århus, Thursday 24<sup>th</sup> November 2016



# Introduction to Numerical Optimisation

What should I minimise?



- ▶ We always minimise a number (or minimise the negative of a number - maximising).
- ▶ This number can be created in any way - it is only a metric (although it can have a physical significance).
- ▶ Minimising many variables can be equivalent to minimising the sum of those elements (usually with normalisation i.e an average).
- ▶ Usually, we minimise this metric as the output of a function.
- ▶ These functions can be “physics” or even “a black-box machine”.
- ▶ Essentially - we can treat any well behaved function as a “black-box” - with only inputs and outputs seen by the optimisation algorithm.

## Finding a minimum

- ▶ A condition for minimisation is the  $\Delta J = J(\mathbf{c}_{s+1}) - J(\mathbf{c}_s) > 0$
- ▶ Taylor series approximated to second order.
  - ▶ If  $J$  is continuously differentiable

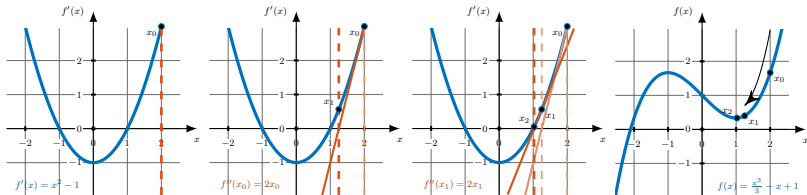
$$\Delta J = J(\mathbf{c}_{s+1}) - J(\mathbf{c}_s) \approx \langle \nabla J_s | \mathbf{c}_s \rangle$$

- ▶ If  $J$  is twice continuously differentiable

$$\Delta J = J(\mathbf{c}_{s+1}) - J(\mathbf{c}_s) \approx \langle \nabla J_s | \mathbf{c}_s \rangle + \frac{1}{2} \langle \mathbf{c}_s | \nabla^2 J_s | \mathbf{c}_s \rangle$$

- ▶ 1st order necessary condition:  $\nabla J_s \Big|_{\min} = 0$
- ▶ 2nd order necessary condition:  $\nabla^2 J_s \Big|_{\min}$  is positive semidefinite

### Finding a minimum to the function using tangents of the gradient





- ▶ **Gradient Descent** Step in direction opposite to local gradient.

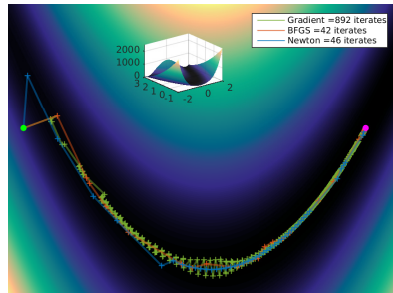
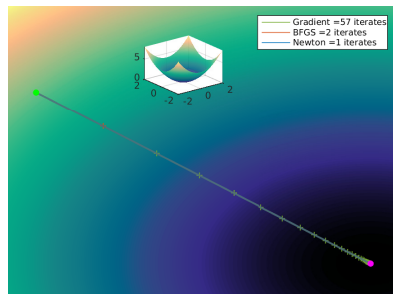
$$J(\mathbf{c}_s + \Delta \mathbf{c}) = J(\mathbf{c}_{s+1}) = J(\mathbf{c}_s) + \langle \nabla J_s | \mathbf{c}_s \rangle$$

- ▶ **Newton-Raphson** Quadratic approximation of objective function, moving to this minimum.

$$J(\mathbf{c}_{s+1}) = J(\mathbf{c}_s) + \langle \nabla J_s | \mathbf{c}_s \rangle + \frac{1}{2} \langle \mathbf{c}_s | \nabla^2 J_s | \mathbf{c}_s \rangle$$

- ▶ **Quasi-Newton BFGS** Approximate  $\nabla^2 J_s$  with information from the gradient history.

$$\nabla^2 J_{s+1} = \nabla^2 J_s + \frac{|\nabla J_s\rangle \langle \nabla J_s|}{\langle \nabla J_s | \mathbf{c}_s \rangle} - \frac{\nabla^2 J_s | \mathbf{c}_s \rangle \langle \mathbf{c}_s | \nabla^2 J_s}{\langle \mathbf{c}_s | \nabla^2 J_s | \mathbf{c}_s \rangle}$$



# Introduction to Optimal Control

- ▶ The Schrödinger equation:

$$\frac{\partial}{\partial t} |\psi(t)\rangle = -\hat{\mathcal{H}} |\psi(t)\rangle$$

- ▶ solved in the static and dynamic case:

*Static:*  $\Rightarrow$

$$|\psi(t)\rangle = \exp\left[-i\hat{\mathcal{H}}t\right] |\psi(0)\rangle$$

*Dynamic:*  $\Rightarrow$

$$|\psi(t)\rangle = \exp_{(o)}\left[-i\int_0^t \hat{\mathcal{H}}(t) dt\right] |\psi(0)\rangle$$

- ▶ Density operator  $\hat{\rho} = |\psi\rangle\langle\psi|$
- ▶ Liouville-von Neumann equation:

$$\begin{aligned}\frac{\partial}{\partial t} \hat{\rho} &= \frac{\partial}{\partial t} (|\psi\rangle\langle\psi|) \\ &= \left(\frac{\partial}{\partial t} |\psi\rangle\right) |\psi\rangle\langle\psi| + |\psi\rangle\langle\psi| \left(\frac{\partial}{\partial t} \langle\psi|\right) \\ &= -i\hat{\mathcal{H}} |\psi\rangle\langle\psi| + i |\psi\rangle\langle\psi| \hat{\mathcal{H}} \\ &= -i \left(\hat{\mathcal{H}}\hat{\rho} - \hat{\rho}\hat{\mathcal{H}}\right) \\ &= -i \left[\hat{\mathcal{H}}, \hat{\rho}\right] \\ &= -i\hat{\mathcal{H}}\hat{\rho}\end{aligned}$$

Dynamic solution to the Liouville-von Neumann equation with the superoperator formalism:

$$\hat{\rho}(t) = \exp_{(o)}\left[-i\int_0^t \hat{\mathcal{H}}(t) dt\right] \hat{\rho}(0)$$

- ▶ The solution to the Liouville-von Neumann equation can be written with vector representation of the density operator

$$|\rho(t)\rangle = \exp_{(\circ)} \left[ -i \int_0^t \hat{\mathcal{H}}(t) dt \right] |\rho(0)\rangle$$

- ▶ The Hamiltonian split into uncontrollable and controllable parts:

$$\hat{\mathcal{H}}(t) = \hat{\mathcal{H}}_0 + \hat{\mathcal{H}}_1(t) + i\hat{\mathcal{R}}$$

- ▶ Controllable part consists of *control channels*:

$$\hat{\mathcal{H}}_1(t) = \sum_{k=1}^K c_k(t) \hat{\mathcal{H}}_k$$

- ▶ *Control channels* are time-independent, and their associated coefficients, *control amplitudes*, are time-dependant.

- ▶ *Control amplitudes* are discretized on a finite grid of time points to obtain *control sequences*:

$$c_k(t) \longrightarrow \vec{c}_k = [c_k(t_1) \quad c_k(t_2) \quad \cdots \quad c_k(t_N)]$$

- ▶ The time-ordered exponential in the solution to the Liouville-von Neumann equation becomes

$$\prod_n \exp \left[ -i \left( \hat{\mathcal{H}}_0 + \sum_{k=1}^K c_{k,n} \hat{\mathcal{H}}_k + i\hat{\mathcal{R}} \right) \Delta t \right]$$

- ▶ where propagation over a single time slice is (ignoring relaxation)

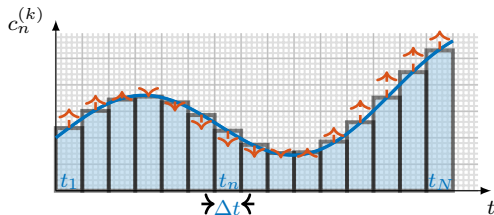
$$\hat{\mathcal{P}}_n = \exp \left[ -i \left( \hat{\mathcal{H}}_0 + \sum_{k=1}^K c_{k,n} \hat{\mathcal{H}}_k \right) \Delta t \right]$$

## Gradient assisted pulse engineering (GRAPE)

- ▶ The aim of quantum optimal control is to *maximise* the fidelity measure, being the overlap between two states:

$$J = \langle \delta | \exp_{(0)} \left[ -i \int_0^T \hat{\mathcal{H}}_0 + \sum_{k=1}^K c_k(t) \hat{\mathcal{H}}_k + i \hat{\mathcal{R}}(t) dt \right] | \rho_0 \rangle$$

### PIECEWISE CONSTANT APPROXIMATION IN A GRAPE SIMULATION



$$\left\langle \text{DESIRED STATE} \left| \hat{\mathcal{P}}_N \hat{\mathcal{P}}_{N-1} \cdots \hat{\mathcal{P}}_2 \hat{\mathcal{P}}_1 \right| \text{INITIAL STATE} \right\rangle$$

- ▶ Initial publications of the GRAPE algorithm used the steepest descent algorithm to minimise  $1 - J$ .
- ▶ The gradient was calculated with finite difference methods
- ▶ These algorithms were advanced to Quasi-Newton optimisation, using the gradient history to find an approximation to the Hessian matrix - giving super-linear convergence.
- ▶ Gradient found from forward and backward propagation:

$$J = \langle \delta | \hat{\mathcal{P}}_N \hat{\mathcal{P}}_{N-1} \hat{\mathcal{P}}_{N-2} \hat{\mathcal{P}}_{N-3} \underbrace{\hat{\mathcal{P}}_{N-4} \dots \hat{\mathcal{P}}_3 \hat{\mathcal{P}}_2 \hat{\mathcal{P}}_1}_{\text{(I) propagate forwards from source}} | \rho_0 \rangle$$

$$\frac{\partial}{\partial c_{k,N-3}} \hat{\mathcal{P}}_{N-3}$$

(III) compute expectation of the derivative

$$J = \langle \delta | \underbrace{\hat{\mathcal{P}}_N \hat{\mathcal{P}}_{N-1} \hat{\mathcal{P}}_{N-2}}_{\text{(II) propagate backwards from target}} \hat{\mathcal{P}}_{N-3} \hat{\mathcal{P}}_{N-4} \dots \hat{\mathcal{P}}_3 \hat{\mathcal{P}}_2 \hat{\mathcal{P}}_1 | \rho_0 \rangle$$

“*nineteen dubious way to compute the exponential of a matrix*”.

**Taylor series** - concerning the error of truncating the arithmetic from roundoff error of floating point arithmetic,  $\epsilon$ ; increasing as  $t\|A\|$  increases.

**Padé approximation** - Again, roundoff error can make this method unreliable. Also, unreliability occurs when  $A$  has widely spread eigenvalues.

**Scaling and squaring** - Exploits the relationship  $e^A = (e^{A/m})^m$  choosing  $m$  to be the smallest power of 2 for which  $\|A\|/m \leq 1$ . Can be used together with the Padé approximation (or Taylor series method).

**Chebyshev rational approximation** -  $c_{qq}(x)$  is the ratio of two polynomials of degree  $q$ . A minimizer for  $\|c_{qq}(A) - e^A\|$  can be found from coefficients given (Cody 69). This is a useful method for sparse matrices.

**Other methods** Ordinary differential equation methods; Polynomial methods; Matrix decomposition methods... Particularly interesting in is Van Loan's investigation of integrals and differentials involving the matrix exponential.

[4] C. Moler and C. Van Loan. In: *SIAM review* 20.4 (1978), pp. 801–836.

[5] W. Cody, G Meinardus and R. Varga. In: *Journal of Approximation Theory* 2.1 (1969), pp. 50–65.

[6] C. Kallstrom. In: *Lund Instit. Technol., Div. Automatic Control, Rep 7309* (1973).

[7] C. F. Van Loan. In: *Automatic Control, IEEE Transactions on* 23.3 (1978), pp. 395–404.

# Auxiliary Matrix Formalism



- ▶ Among the many complicated functions encountered in magnetic resonance simulation context, chained exponential integrals involving square matrices  $\mathbf{A}_k$  and  $\mathbf{B}_k$  occur particularly often:

$$\int_0^t dt_1 \int_0^{t_1} dt_2 \cdots \int_0^{t_{n-2}} dt_{n-1} \left\{ e^{\mathbf{A}_1(t-t_1)} \mathbf{B}_1 e^{\mathbf{A}_2(t_1-t_2)} \mathbf{B}_2 \cdots e^{\mathbf{A}_1(t-t_1)} \mathbf{B}_{n-1} e^{\mathbf{A}_n t_{n-1}} \right\}$$

- ▶ A method for computing some of the integrals of the general type shown in Equation of this type was proposed by Van Loan in 1978 (pointed out by Sophie Schirmer)
- ▶ Using this augmented exponential technique, we can write an upper-triangular block matrix exponential as

$$\exp \begin{pmatrix} \mathbf{A} & \mathbf{B} \\ \mathbf{0} & \mathbf{A} \end{pmatrix} = \begin{pmatrix} e^{\mathbf{A}t} & \int_0^t e^{\mathbf{A}(t-s)} \mathbf{B} e^{\mathbf{A}s} ds \\ \mathbf{0} & e^{\mathbf{A}t} \end{pmatrix} = \begin{pmatrix} e^{\mathbf{A}} & \int_0^1 e^{\mathbf{A}(1-s)} \mathbf{B} e^{\mathbf{A}s} ds \\ \mathbf{0} & e^{\mathbf{A}} \end{pmatrix}$$

## Auxiliary Matrix Formalism

- ▶ Find the derivative of the control pulse at a specific time point
- ▶ set

$$\int_0^1 e^{\mathbf{A}(1-s)} \mathbf{B} e^{\mathbf{A}s} ds = D_{c_n}(t) \exp(-i\hat{\mathcal{L}}\Delta t) \Rightarrow \mathbf{B} = -i\hat{\mathcal{H}}_k \Delta t$$

- ▶ where  $\hat{\mathcal{L}} = \hat{\mathcal{H}}_0 + \sum_k c_{k,n} \hat{\mathcal{H}}_k$ .
- ▶ This leads to an efficient calculation of a gradient element

$$\exp \begin{pmatrix} -i\hat{\mathcal{L}}\Delta t & -i\hat{\mathcal{H}}_{k,n} \Delta t \\ \mathbf{0} & -i\hat{\mathcal{L}}\Delta t \end{pmatrix} = \begin{pmatrix} e^{-i\hat{\mathcal{L}}\Delta t} & \frac{\partial}{\partial c_{k,n}} e^{-i\hat{\mathcal{L}}\Delta t} \\ \mathbf{0} & e^{-i\hat{\mathcal{L}}\Delta t} \end{pmatrix}$$

- ▶ This auxiliary matrix formalism can also be applied to other areas of magnetic resonance:
  - ▶ average Hamiltonian theory following interaction representation transformations
  - ▶ Bloch-Redfield-Wangsness theory of nuclear and electron relaxation

- ▶ Can use augmented exponential with Krylov propagation

$$\exp \begin{pmatrix} -i\hat{\mathcal{L}}\Delta t & -i\hat{\mathcal{H}}_{k,n}\Delta t \\ \mathbf{0} & -i\hat{\mathcal{L}}\Delta t \end{pmatrix} \begin{pmatrix} \mathbf{0} \\ \rho_n \end{pmatrix} \Rightarrow \begin{pmatrix} \frac{\partial}{\partial c_{k,n}} e^{-i\hat{\mathcal{L}}\Delta t} \\ \mathbf{0} \end{pmatrix}$$

- ▶ We need  $n$  of these Krylov propagations, plus  $2n$  Krylov propagations from the fidelity calculation (forwards and backwards to each  $n$ ) to calculate the gradient element

$$\nabla J(c_{k,n}) = (\rho_{n+1} \quad \mathbf{0}) \begin{pmatrix} \frac{\partial}{\partial c_{k,n}} e^{-i\hat{\mathcal{L}}\Delta t} \\ \mathbf{0} \end{pmatrix}$$

- ▶ If Krylov propagation is not appropriate, Spinach will calculate the explicit propagators with the matrix exponential of our auxiliary matrix.
- ▶ Particularly, we use the Taylor method (with gpu calculation if available), and preserve sparsity with a matrix cleanup during the iterative algorithm (remove any elements  $< 10^{-14}$ )

# Quadratic convergence

The Newton step:  $p_s^N = -\mathbf{H}_s^{-1} \nabla J_s$

- ▶  $\mathbf{H}_s = \nabla^2 J_s$  is the Hessian matrix, one of second order partial derivatives:

$$\mathbf{H} = \begin{pmatrix} \frac{\partial^2 J}{\partial c_1^2} & \frac{\partial^2 J}{\partial c_1 \partial c_2} & \cdots & \frac{\partial^2 J}{\partial c_1 \partial c_m} \\ \frac{\partial^2 J}{\partial c_2 \partial c_1} & \frac{\partial^2 J}{\partial c_2^2} & \cdots & \frac{\partial^2 J}{\partial c_2 \partial c_m} \\ \vdots & \vdots & \ddots & \vdots \\ \frac{\partial^2 J}{\partial c_m \partial c_1} & \frac{\partial^2 J}{\partial c_m \partial c_2} & \cdots & \frac{\partial^2 J}{\partial c_m^2} \end{pmatrix}$$

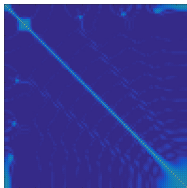
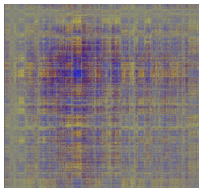
- ▶ The steepest descent method results from the same equation when we set  $\mathbf{H}$  to the identity matrix.
- ▶ Quasi-Newton methods initialise  $\mathbf{H}$  to the identity matrix, then to approximate it from an update formula using a gradient history.
- ▶ The Hessian proper must be positive definite (and quite well conditioned) to make an inverse; an indefinite Hessian results in non-descent search directions.

- ▶ (block) off-diagonal elements:

$$\frac{\partial^2 J}{\partial c_{k,n_2} \partial c_{k,n_1}} = \langle \delta | \hat{\mathcal{P}}_N \hat{\mathcal{P}}_{N-1} \cdots \frac{\partial}{\partial c_{k,n_2}} \hat{\mathcal{P}}_{n_2} \cdots \frac{\partial}{\partial c_{k,n_1}} \hat{\mathcal{P}}_{n_1} \cdots \hat{\mathcal{P}}_2 \hat{\mathcal{P}}_1 | \rho_0 \rangle$$

- ▶ All propagators of the non-diagonal blocks have been calculated within a gradient calculation, and can be reused.
- ▶ Only need to find the diagonal blocks.
- ▶ (block) diagonal elements:

$$\frac{\partial^2 J}{\partial c_{k,n}^2} = \langle \delta | \hat{\mathcal{P}}_N \hat{\mathcal{P}}_{N-1} \cdots \frac{\partial^2}{\partial c_{k,n}^2} \hat{\mathcal{P}}_n \cdots \hat{\mathcal{P}}_2 \hat{\mathcal{P}}_1 | \rho_0 \rangle$$



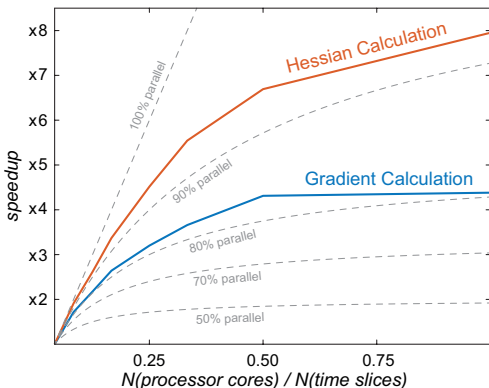
- ▶ second order derivatives can be calculated with a  $3 \times 3$  augmented exponential
- ▶ set

$$\int_0^1 \int_0^s e^{\mathbf{A}(1-s)} \mathbf{B}_{n_1} e^{\mathbf{A}(s-r)} \mathbf{B}_{n_2} e^{\mathbf{A}r} dr ds = D_{c_{n_1} c_{n_2}}^2(t) \exp(-i\hat{\mathcal{L}}\Delta t) \Rightarrow \mathbf{B}_n = -i\hat{\mathcal{H}}_{k,n} \Delta t$$

- ▶ Giving the efficient Hessian element calculation

$$\exp \begin{pmatrix} -i\hat{\mathcal{L}}\Delta t & -i\hat{\mathcal{H}}_{k_1,n_1} \Delta t & 0 \\ 0 & -i\hat{\mathcal{L}}\Delta t & -i\hat{\mathcal{H}}_{k_2,n_2} \Delta t \\ 0 & 0 & -i\hat{\mathcal{L}}\Delta t \end{pmatrix} =$$

$$\begin{pmatrix} e^{-i\hat{\mathcal{L}}\Delta t} & \frac{\partial}{\partial c_{k_1,n_1}} e^{-i\hat{\mathcal{L}}\Delta t} & \frac{1}{2} \frac{\partial^2}{\partial c_{k_1,n_1} \partial c_{k_2,n_2}} e^{-i\hat{\mathcal{L}}\Delta t} \\ 0 & e^{-i\hat{\mathcal{L}}\Delta t} & \frac{\partial}{\partial c_{k_2,n_2}} e^{-i\hat{\mathcal{L}}\Delta t} \\ 0 & 0 & e^{-i\hat{\mathcal{L}}\Delta t} \end{pmatrix}$$



- ▶ Amdahl's law: parallelisation efficiency analysis for the Hessian calculation compared to the gradient calculation within Spinach implementation of GRAPE. The optimal control problem involves 24 time slices and 6 control channels, yielding a fidelity functional gradient with 144 elements and a  $144 \times 144$  Hessian.



# Hessian Regularisation

- ▶ Common when we have negative eigenvalues, regularise the Hessian to be positive definite.
- ▶ Check if positive definite by attempting a Cholesky factorisation of the Hessian matrix:

$$\mathbf{H} = \mathbf{L}\mathbf{L}^T \Rightarrow \mathbf{H}^{-1} = (\mathbf{L}^{-1})^T \mathbf{L}^{-1}$$

- ▶ Naive method to revert to gradient descent, with  $\mathbf{H} = \mathbf{1}$ , when indefinite Hessian is encountered
- ▶ Indefinite Hessian becomes very common with increased problem dimension - optimiser will spend most time as gradient descent.
- ▶ Alternatively an iterative method using trial values of a constant summed to the Hessian diagonal, until a Cholesky factorisation succeeds.

$$\mathbf{H} + \sigma \mathbf{1} = \mathbf{L}\mathbf{L}^{-1}, \quad \sigma \geq 0$$

$$\sigma = \begin{cases} \|\mathbf{H}\|_F - \min [\mathbf{H}]_{ii} & \text{if } \min [\mathbf{H}]_{ii} < 0 \\ \|\mathbf{H}\|_F & \text{if } \min [\mathbf{H}]_{ii} \geq 0 \end{cases}$$

## Trust Region Method & Rational Function Optimisation

- ▶ More sophisticated to add the smallest negative eigenvalue to all eigenvalues, then reform the Hessian with initial eigenvectors:

$$\mathbf{H} = \mathbf{Q}\mathbf{\Lambda}\mathbf{Q}^{-1}$$

$$\lambda_{\min} = \max [0, -\min(\mathbf{\Lambda})]$$

$$\mathbf{H}_{\text{reg}} = \mathbf{Q}(\mathbf{\Lambda} + \lambda_{\min}\mathbf{1})\mathbf{Q}^{-1}$$

- ▶ **TRM** Introduce a constant  $\delta$ ; region of a radius we trust to give a sufficiently positive definite Hessian.

$$\mathbf{H}_{\text{reg}} = \mathbf{Q}(\mathbf{\Lambda} + \delta\lambda_{\min}\mathbf{1})\mathbf{Q}^{-1}$$

However, if  $\delta$  is too small, the Hessian will become ill-conditioned.

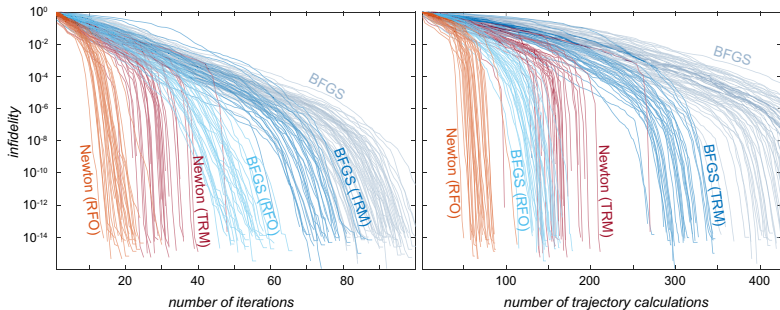
- ▶ **RFO** The method proceeds to construct an augmented Hessian matrix

$$\mathbf{H}_{\text{aug}} = \begin{bmatrix} \alpha^2\mathbf{H} & \alpha\langle\nabla J_s\rangle \\ \alpha\langle\nabla J_s| & \mathbf{0} \end{bmatrix} = \mathbf{Q}\mathbf{\Lambda}\mathbf{Q}^{-1}$$

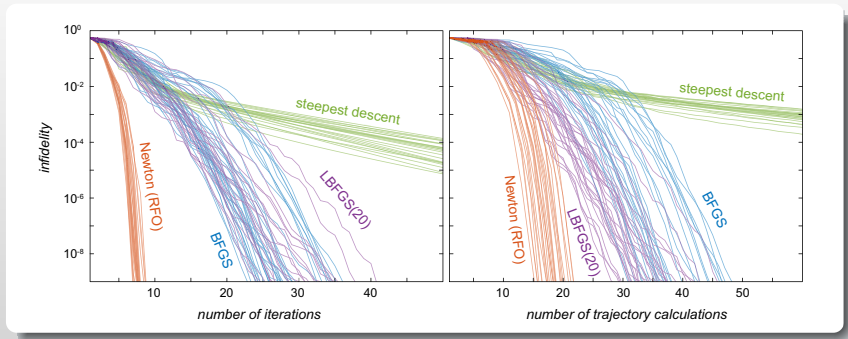
$$\sigma = \max [0, -\min(\mathbf{\Lambda})]$$

$$\mathbf{H}_{\text{reg}} = \frac{1}{\alpha^2}\mathbf{Q}(\mathbf{\Lambda} + \sigma\mathbf{1})\mathbf{Q}^{-1}$$

This method can proceed iteratively, reducing  $\alpha$  each time until the condition number of the matrix is less than a defined bound.



- ▶ State transfer in an H–C–F group in a 9.4 Tesla magnet with  $^1\text{H}$  isotope for hydrogen,  $^{13}\text{C}$  isotope for carbon and  $^{19}\text{F}$  isotope for fluorine, with the  $^1\text{H}$ – $^{13}\text{C}$  J-coupling of 140 Hz,  $^{13}\text{C}$ – $^{19}\text{F}$  J-coupling of –160 Hz and all three signals assumed to be on resonance with the transmitters on the corresponding NMR spectrometer channels. A six-channel  $\{H_X, H_Y, C_X, C_Y, F_X, F_Y\}$  shaped pulse with a duration of 100 ms, a quadratic penalty for excursions outside the 10 kHz power envelope and 50 time discretisation points was optimized to perform longitudinal magnetization transfer from  $^1\text{H}$  to  $^{19}\text{F}$ .

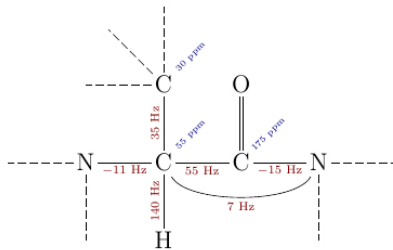
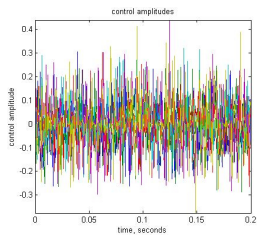
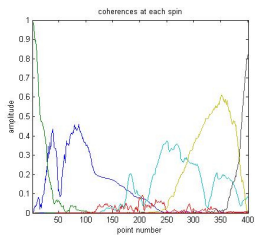
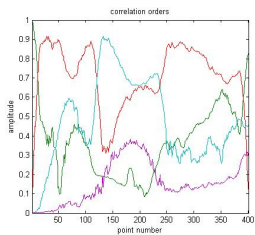


- ▶ State transfer from longitudinal polarization into a two-spin singlet state, while allowing for up to 20% miscalibration of the control channel power level. The spin system contains two  $^{13}\text{C}$  spins in a 14.1 Tesla magnet with chemical shifts of 0.00 and 0.25 ppm and a J-coupling of 60 Hz. The system is prepared in the  $C_Z^{(1)} + C_Z^{(2)}$  state and a two-channel control sequence on  $C_X^{(1)} + C_X^{(2)}$  and  $C_X^{(1)} + C_X^{(2)}$  control operators with 50 time discretization points, the nominal power of 60 Hz and the duration of 50 milliseconds is optimized simultaneously for ten different power levels spaced equally between 80

# Experimental work

# Larger systems

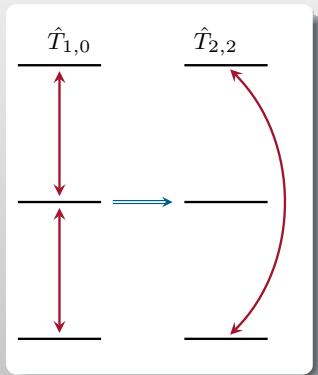
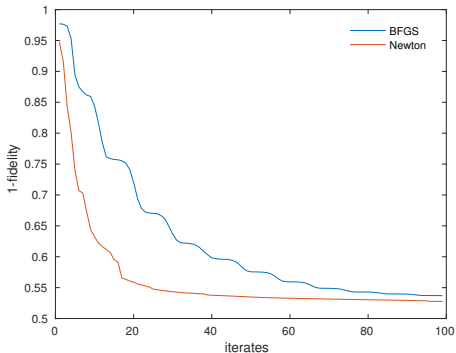
## Simulation



# Overtone excitation

## Simulation

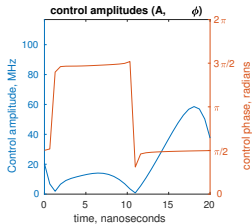
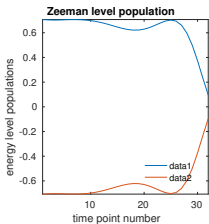
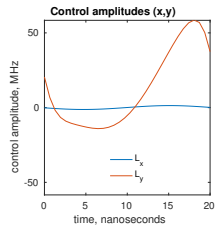
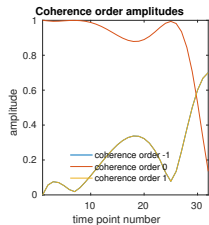
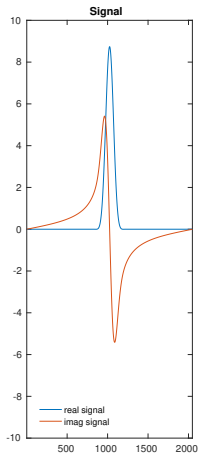
- ▶ Excite  $^{14}\text{N}$  from a state  $\hat{T}_{1,0} \rightarrow \hat{T}_{2,2}$ .
- ▶ Solid state powder average, with objective functional weighted over the crystalline orientations (rank 17 Lebedev grid - 110 points).
- ▶ Nuclear quadrupolar interaction.
- ▶ 400 time points for total pulse duration of  $40\mu\text{s}$





# Simple optimised echo

$B_0$  Inhomogeneity



An Actual Laboratory!

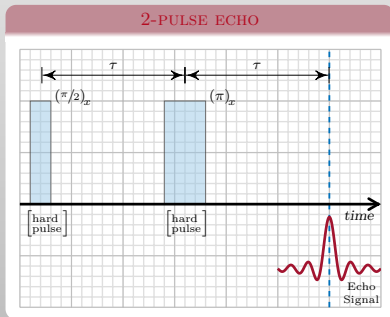


# Optimising an Experiment

## Using PulseSPEL variables

- ▶ matlab function forms the objective function of an optimisation algorithm
- ▶ python scripts are invoked by matlab, using data saved by matlab
- ▶ commands sent to modify PulseSPEL files from python a script
- ▶ send new PulseSPEL variables to experiment and run the experiment with another python script
- ▶ read the signal produced from these new variables

- ▶ Simple, 2-pulse echo experiment.
- ▶ Aim to find an optimised echo.
- ▶ Maximise the area under the real part of the echo signal.
- ▶ Vary the time between pulses,  $\tau$ .



```
; FT-EPR package
;
; PulseSPEL variable
; definitions & conventions
begin defs

; Variables ; Comments:

p0 = 16 ; 90 pulse length
p1 = 32 ; 180 pulse length
p4 = 100 ; laser trigger

d0 = 400 ; Acquisition delay
d1 = 260 ; tau

aa0 = 13 ; amplitude
aa1 = 20 ;

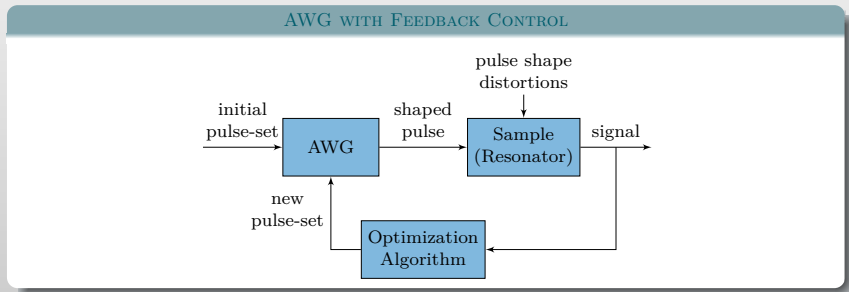
ap11 = 0 ; phase pulse 1
ap12 = 180 ;
ap13 = 90 ;
ap14 = 270 ;

ap21 = 0 ; phase pulse 2
ap22 = 180 ;
ap23 = 90 ;
ap24 = 270 ;

as0 = 0 ; AWG pulse shapes
as1 = 83 ;
end defs
```

- ▶ Newton based methods have good convergence properties, but all need a gradient.
- ▶ Gradient-free optimisation can make an estimate of the gradient through finite differences - but this is usually expensive with little or no gains from an inexact gradient.
- ▶ Simplex methods find better points at each iterate - but convergence is not guaranteed.
- ▶ Simplex methods do not work well with bounds.
- ▶ Most optimisation methods work on smooth function.
- ▶ Optimising an integer variable digitises the surface, potentially creating false stationary points.

- ▶ The AWG can shape the phase and amplitude of a pulse.
- ▶ The sent shaped pulse may not be exactly what the experiment sees - may need to create a response function.



[20] P. E. Spindler, Y. Zhang, B. Endeward, N. Gershernzon, T. E. Skinner, S. J. Glaser and T. F. Prisner. In: *J. Magn. Reson.* 218 (2012), pp. 49–58.

[21] P. E. Spindler, S. J. Glaser, T. E. Skinner and T. F. Prisner. In: *Angewandte Chemie International Edition* 52.12 (2013), pp. 3425–3429.

[22] T. Kaufmann, T. J. Keller, J. M. Franck, R. P. Barnes, S. J. Glaser, J. M. Martinis and S. Han. In: *J. Magn. Reson.* 235 (2013), pp. 95–108.

[23] A. Doll, S. Pribitzer, R. Tschaggelar and G. Jeschke. In: *J. Magn. Reson.* 230 (2013), pp. 27–39.

[24] A. Doll and G. Jeschke. In: *J. Magn. Reson.* 246 (2014), pp. 18–26.

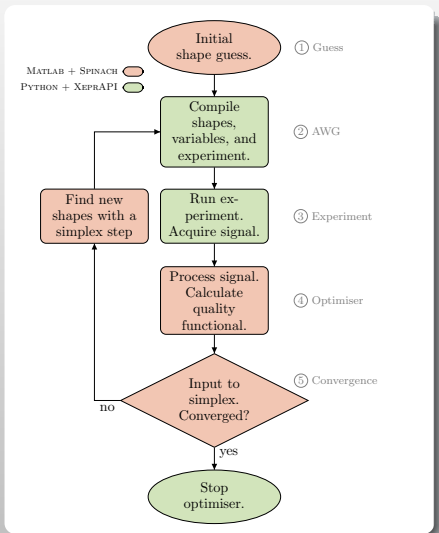
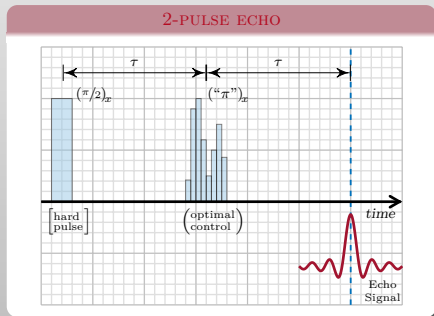
[25] P. Schöps, P. E. Spindler, A. Marko and T. F. Prisner. In: *J. Magn. Reson.* 250 (2015), pp. 55–62.

[26] G. Jeschke, S. Pribitzer and A. Doll. In: *The Journal of Physical Chemistry B* 119.43 (2015), pp. 13570–13582.

# Optimising an Echo

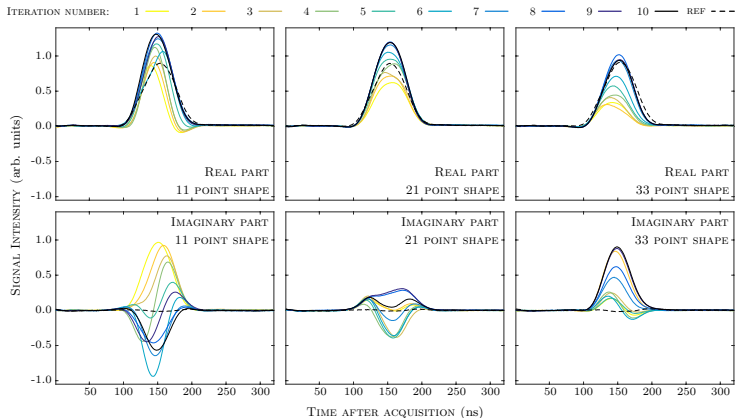
## Using a Shaped Waveform

- ▶ Simple, 2-pulse echo experiment.
- ▶ Aim to find an optimised echo.
- ▶ Maximise the area under the real part of the echo signal.
- ▶ Vary the shape of the soft  $\pi$ -pulse.
- ▶ Many pulses take a long time to optimise (as opposed to a chirped pulse which have only 3 or 4 variables to optimise)



# Optimising an Echo

## Using a Shaped Waveform



Real (top) and imaginary (bottom) parts of the echo signal at improved iterations. Results are shown for three different forms of a shape file (shown from left to right) with 11, 21, and 33 points defining shape for each control channel. Experiment performed on a simple nitroxide system. The first 10 iterations show the fastest progress in finding an optimal solution. Function evaluations for plots (left to right) are 119, 325, and 341 respectively

- ▶ Another measure to optimise could be the shape of the signal.
- ▶ Requires a reference shape, that which we would like the signal to mimic.
- ▶ Optimise:  $\langle \text{REFERENCE PLOT} | \text{CURRENT PLOT} \rangle$

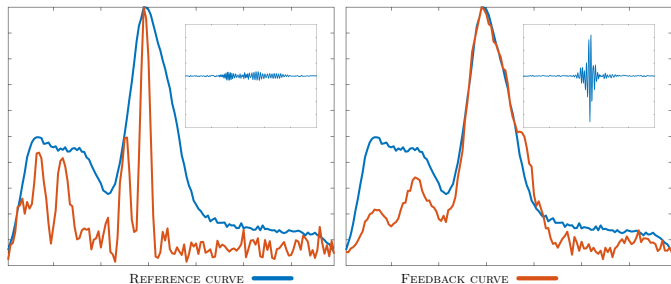


Diagram of curve matching from an echo signal (signals shown inset with the same arbitrary scales) - (left) after 1 optimisation iterate, (right) after 50 iterates. The direct measurement feedback loop is based on a broadband echo experiment using 2 optimised CHIRPS. The Fourier transform of the echo signal is matched to a reference from a field sweep experiment.



- ▶ Ilya Kuprov (Southampton)
- ▶ Sean Wright (Southampton)
- ▶ Marina Carravetta (Southampton)
- ▶ Phil Williamson (Southampton)
- ▶ Maria Concistre (Southampton)
- ▶ Peppe Pileio (Southampton)
- ▶ William Myers (Oxford)
- ▶ Christiane Timmel (Oxford)
- ▶ Arzhang Ardavan (Oxford)
- ▶ Stefan Glaser (München)
- ▶ Thomas Schulte-Herbrüggen (München)
- ▶ Ville Bergholm (München)
- ▶ Sophie Schirmer (Swansea)
- ▶ Mads Sloth Vinding (Århus)

### FUNDING

This work is supported by a funding from QUAINT EU FP7, EPSRC iMR-CDT doctoral training centre.

## REFERENCES

- [1] W. Cody, G. Meinardus and R. Varga. 'Chebyshev rational approximations to  $\exp(-x)$  in  $[0, +\infty]$  and applications to heat-conduction problems'. In: *Journal of Approximation Theory* 2.1 (1969), pp. 50–65.
- [2] A. Doll and G. Jeschke. 'Fourier-transform electron spin resonance with bandwidth-compensated chirp pulses'. In: *J. Magn. Reson.* 246 (2014), pp. 18–26.
- [3] A. Doll, S. Pribitzer, R. Tschaggelar and G. Jeschke. 'Adiabatic and fast passage ultra-wideband inversion in pulsed EPR'. In: *J. Magn. Reson.* 230 (2013), pp. 27–39.
- [4] F. F. Floether, P. de Fouquieres and S. G. Schirmer. 'Robust quantum gates for open systems via optimal control: Markovian versus non-Markovian dynamics'. In: *New Journal of Physics* 14.7 (2012), p. 073023.
- [5] P. de Fouquieres, S. Schirmer, S. Glaser and I. Kuprov. 'Second order gradient ascent pulse engineering'. In: *Journal of Magnetic Resonance* 212.2 (2011), pp. 412–417.
- [6] D. L. Goodwin and I. Kuprov. 'Auxiliary matrix formalism for interaction representation transformations, optimal control, and spin relaxation theories'. In: *The Journal of Chemical Physics* 143.8 (2015), p. 084113.
- [7] D. L. Goodwin and I. Kuprov. 'Modified Newton-Raphson GRAPE methods for optimal control of spin systems'. In: *The Journal of Chemical Physics* 144.20 (2016), p. 204107.
- [8] G. Jeschke, S. Pribitzer and A. Doll. 'Coherence transfer by passage pulses in electron paramagnetic resonance spectroscopy'. In: *The Journal of Physical Chemistry B* 119.43 (2015), pp. 13570–13582.
- [9] C. Kallstrom. 'Computing  $\exp(A)$  and  $\int \exp(As) ds$ '. In: *Lund Instit. Technol., Div. Automatic Control, Rep 7309* (1973).
- [10] T. Kaufmann, T. J. Keller, J. M. Franck, R. P. Barnes, S. J. Glaser, J. M. Martinis and S. Han. 'DAC-board based X-band EPR spectrometer with arbitrary waveform control'. In: *J. Magn. Reson.* 235 (2013), pp. 95–108.
- [11] N. Khaneja, T. Reiss, C. Kehlet, T. Schulte-Herbrüggen and S. J. Glaser. 'Optimal control of coupled spin dynamics: design of NMR pulse sequences by gradient ascent algorithms'. In: *Journal of Magnetic Resonance* 172.2 (2005), pp. 296–305.
- [12] C. Moler and C. Van Loan. 'Nineteen dubious ways to compute the exponential of a matrix'. In: *SIAM review* 20.4 (1978), pp. 801–836.
- [13] I. Najfeld and T. F. Havel. 'Derivatives of the Matrix Exponential and Their Computation'. In: *Advances in Applied Mathematics* 16.3 (1995), pp. 321–375.
- [14] P. Schöps, P. E. Spindler, A. Marko and T. F. Prisner. 'Broadband spin echoes and broadband SIFTER in EPR'. In: *J. Magn. Reson.* 250 (2015), pp. 55–62.
- [15] P. E. Spindler, S. J. Glaser, T. E. Skinner and T. F. Prisner. 'Broadband inversion PELDOR spectroscopy with partially adiabatic shaped pulses'. In: *Angewandte Chemie International Edition* 52.12 (2013), pp. 3425–3429.
- [16] P. E. Spindler, Y. Zhang, B. Endeward, N. Gershenson, T. E. Skinner, S. J. Glaser and T. F. Prisner. 'Shaped optimal control pulses for increased excitation bandwidth in EPR'. In: *J. Magn. Reson.* 218 (2012), pp. 49–58.
- [17] C. F. Van Loan. 'Computing integrals involving the matrix exponential'. In: *Automatic Control, IEEE Transactions on* 23.3 (1978), pp. 395–404.